World Journal of Applied Chemistry
2016; 1(1): 9-15
http://www.sciencepublishinggroup.com/j/wjac
doi: 10.11648/j.wjac.20160101.12

Dye Sensitized TiO_2 Nanopore Thin Films with Antimicrobial Activity Against Methicillin Resistant Staphylococcus Aureus Under Visible Light

P. M. Perillo*, F. C. Getz

National Atomic Energy Commission, Micro and Nanotechnology Group, Buenos Aires, Argentina

Email address:
perillo@cnea.gov.ar (P. M. Perillo)
*Corresponding author

To cite this article:
P. M. Perillo, F. C. Getz. Dye Sensitized TiO_2 Nanopore Thin Films with Antimicrobial Activity Against Methicillin Resistant Staphylococcus Aureus Under Visible Light. *World Journal of Applied Chemistry.* Vol. 1, No. 1, 2016, pp. 9-15.
doi: 10.11648/j.wjac.20160101.12

Received: September 6, 2016; **Accepted**: September 22, 2016; **Published**: October 14, 2016

Abstract: In this work the antimicrobial activity of TiO_2 nanopore thin films sensitized by Copper tetracarboxyphthalocyanines (T_cP_cCu) was investigated. TiO_2 thin films were deposited by magnetron sputtering and the sensitization process was done by adsorption process. The samples were characterized by scanning electronic microscopy (SEM), Fourier Transform infrared spectroscopy (FTIR), UV-Vis spectrophotometry, diffuse reflectance and Raman spectroscopy. Finally, the antimicrobial effect against Methicillin resistant Staphylococcus aureus (MRSA) under visible irradiation on TiO_2 and T_cP_cCu/TiO_2 was studied. The antimicrobial assay showed that T_cP_cCu/TiO_2 thin films reach 80.4% (+/3.4) of inhibition of MRSA growth after visible irradiation.

Keywords: TiO_2 Nanopores, Thin Film, Photodynamic Therapy, MRSA

1. Introduction

In recent years, pathogens have become public threats large-scale, which have been found to have an effect on human's health, food safety and even national security with a considerable economic loss [1, 2]. Staphylococcus aureus (SA) is a dangerous human pathogen, carried by about 30% of the population and a leading etiologic agent of nosocomial and community acquired infectious diseases. As one of the most ubiquitous pathogens in public healthcare worldwide [3, 4], SA has been a major common cause of bloodstream infections, osteomyelitis, endocarditis and toxic shock syndrome [5]. Furthermore it has been reported to persist inside phagocytes for prolonged periods. However, a more thorough characterization of the different mechanisms for intracellular persistence is lacking. It has been showed that protection from primary staphylococcal infection is mainly dependent on innate rather than adaptive immune responses [6]. It is known that SA bacteria are resistant to some conventional antibacterial drugs like penicillin, methicillin and vancomycin. Last years, there were many researches in the field intended to find new alternatives to control this pathogenic microorganisms resistant to antibiotics [7]. Antimicrobial Photodynamic Therapy (APT) is a potential methodology to solve this problem. APT uses three non-toxic components: photo sensitizers, electromagnetic radiation and molecular oxygen $^3O_2$. These three factors generate reactive oxygen species (ROS) which are highly cytotoxic to bacteria [8–10]. In recent years, many practical applications of nanoparticles on APT were found [11]. APT relies in excitation of photosensitizer (PS) under electromagnetic visible radiation in the presence of basal triplet state $^3O_2$, when PS absorbs light; it excites from basal state (^{0}PS) to singlet state (^{1}PS*) after that, two different process can occur: (a) 1PS* could return to ^{o}PS state through fluorescence process or (b) ^{1}PS* could decay to triplet state (^{3}PS*) through internal cross system process; if ^{3}PS* is generated two different process could occur; ^{3}PS* could return to ^{o}PS state through phosphorescence process or 3PS* could react to $^3O_2$ to generate excited singlet state oxygen $^1O_2$; this kind of reaction is known as type II reaction or energy transfer reaction; furthermore, ^{3}PS* also could produce radical species as hydroxyl or superoxide radicals through electron transfer reaction, this kind of reaction is

known as type I; $^1O_2$ is an important ROS and is highly cytotoxic, it can react to a large number of biological substrates [12–18]. Among the semiconductors options; titanium dioxide (TiO_2) has shown good bio-deactivation properties against different microorganism like cyanobacteria and microscopic fungi, viruses, prions and cancer cells [19–21]. Pure TiO_2 is photoactive only under UV irradiation; however, photosensitization with organic and inorganic dyes is a convectional way to shift optical properties of semiconductors to visible range of electromagnetic spectrum [22]. Most photosensitizers used for APT are porphyrins, chlorines and bacteriochlorins; however, phthalocyanines, purpurines and texapirines are investigated as main alternatives [23]. Among these photosensitizers; phthalocyanines are an attractive option, they have high quantum yield of $^1O_2$ production, a high molar absorptivity in the visible range of the electromagnetic spectrum and besides, they have high absorption coefficient in the red region of the spectrum (670 nm) where light can penetrate the tissues and high photostability to minimize the effects of photobleaching [24, 25]. Different phthalocyanines and their derivatives are used in APT application due to possibility to generate large amounts of singlet oxygen and other ROS; cytotoxic species against antibiotic resistant bacteria, especially gram positive bacteria such as SA.

In this work, we studied antimicrobial activity of TiO_2 nanopore thin films sensitized by P_cT_cCu under visible radiation as possible alternative to source antimicrobial material.

2. Experimental Procedure

2.1. Synthesis and Characterizations of Phthalocyanines

The procedure for the synthesis was as follows: copper sulfate (II), trimellitic anhydride, urea, and ammonium chloride were mixed in 10.0 ml of nitrobenzene. The reaction was catalyzed with ammonium tetramolybdate. The mixture was heated to reflux at 185 °C for 4 h. Then, the dye was purified and recrystallized in acid medium [26, 27].

The samples were characterized by scanning electron microscopy (SEM), X-ray diffraction (XRD), UV-Vis spectrophotometry, Fourier Transform Infrared Spectroscopy (FTIR), diffuse reflectance and Raman spectroscopy. A Zeiss Supra40 Gemini microscope was employed for the morphological characterization of the TiO_2 samples.

XRD patterns were recorded with a diffractometer (PANalytical model Empyrean) equipped Cu Kα (λ = 0.15418 nm) using a generator voltage of 40 kV and current of 40 mA. FTIR spectra were recorded in a Nicolet MAGNA 560 instrument equipped with a liquid N_2 cooled MCT-A detector.

The diffuse reflectance absorption spectrum was measured using a Lambda 4 Perkin Elmer spectrophotometer equipped with an integrating sphere. Raman measurements were carried out using a Jovin Yvon T64000 spectrometer equipped with a microscope objective and a charge coupled device detector (CCD).

2.2. Thin Films Sensitization

Ti films (600 nm in thickness) were deposited by RF magnetron sputtering on p-type Si (100) wafer with 300 nm layer of SiO_2. The detailed preparation of TiO_2 thin film nanotubes was reported in our previous work [28]. TiO_2 thin films were immersed in a solution of each phthalocyanine by 16 hours at room temperature and constant stirring, after that, sensitized films were washed and dried.

2.3. Antimicrobial Activity Test

The plate count methodology was used and the viable cells in terms of colony forming units (CFU) were estimated [29, 30].

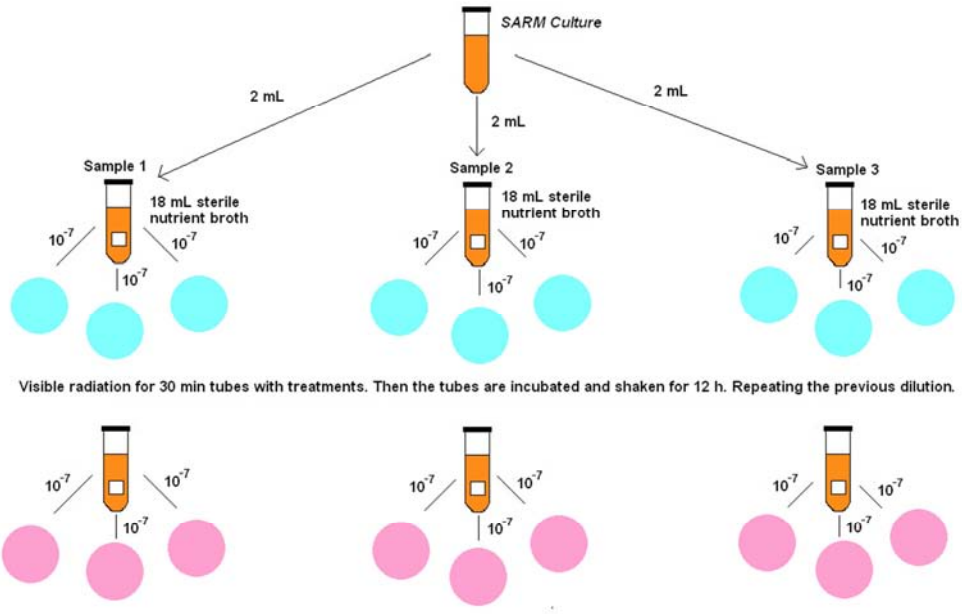

Fig. 1. *UFC counting dishes methodology to inhibition assay of Staphylococcus aureus growth under visible irradiation.*

First, we inoculated strains resistant SA in 30 ml of sterile nutrient broth, and it was stirred for 12 hours at 37°C, after time incubation, optical density of the culture was measured to determinate the respective microorganism growth.

Cultures with same absorbance were prepared at different falcon tubes, a culture was grown without any treatment as the negative control and gentamicin was used as positive control.

Dilution in series until 107 for each crop was used; the thin films were submerged into the crops. The samples were irradiated under visible light (450 μWcm^{-2}) for 30 minutes, after that were incubated and agitated for 12 hours. Procedure was performed by triplicate. Finally, we performed the electronic counting of CFU into petri dishes to determinate antimicrobial activity. Fig. 1 shows general description of antimicrobial test methodology.

3. Results and Discussion

3.1. XRD TiO_2 Thin Film Characterization

The corresponding XRD pattern of TiO_2 nanostructure fabricated from Ti film at 60 V anodizing voltage after being annealed at 550°C is shown in Fig.2. Typical peaks of anatase phase at 2θ near 25°, 37° and 48° are observed, which correspond to planes (101), (004) and (200), respectively. Also typical peaks of rutile phase at 2θ near 27°, 36°, 41° and 54° are observed which correspond to the planes (110), (101), (111) and (211), respectively. The peak at 2θ near 33° belongs to Si (200) plane of the substrate. In summary, the structure consists of a mixed phase of anatase (01-086-1157) and rutile (00-034-0180).

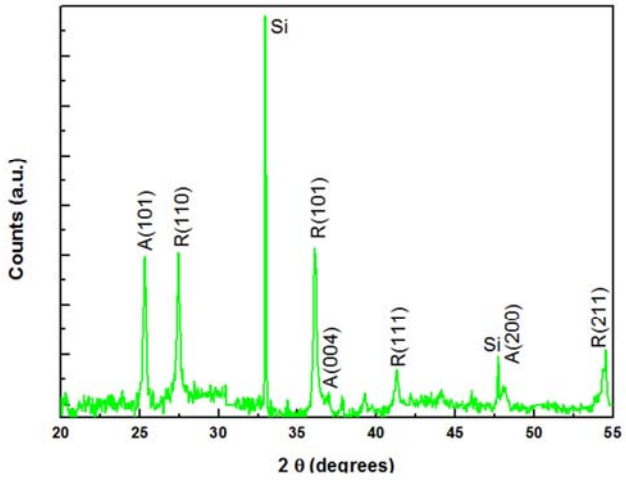

Fig. 2. *XRD patterns of TiO_2 nanostructure prepared on Ti films.*

3.2. FTIR Phthalocyanine Characterization

Fig.3 shows FTIR to T_cP_cCu synthesized in this work. Typical broadband is located between 3418 cm^{-1}, this signal could be assigned to O–H; this broad and strong signal overlapped the signal of chemical bond stretching of N–H.

Aromatic chemical functional groups is corroborated by absorption at 1700–1200 cm^{-1}, signal located at v = 1668 cm^{-1} corresponds to asymmetric stretching of C=O-, strong signal located at v = 1524 cm^{-1} could be assigned to chemical bond stretching of C=C of aromatic groups, signal located at v = 1355 cm^{-1} chemical bond stretching of C–O of carboxylic acid group and besides, signal located near to 1007 cm^{-1} is assigned to chemical bond bending of C–C in aromatic groups [31, 32].

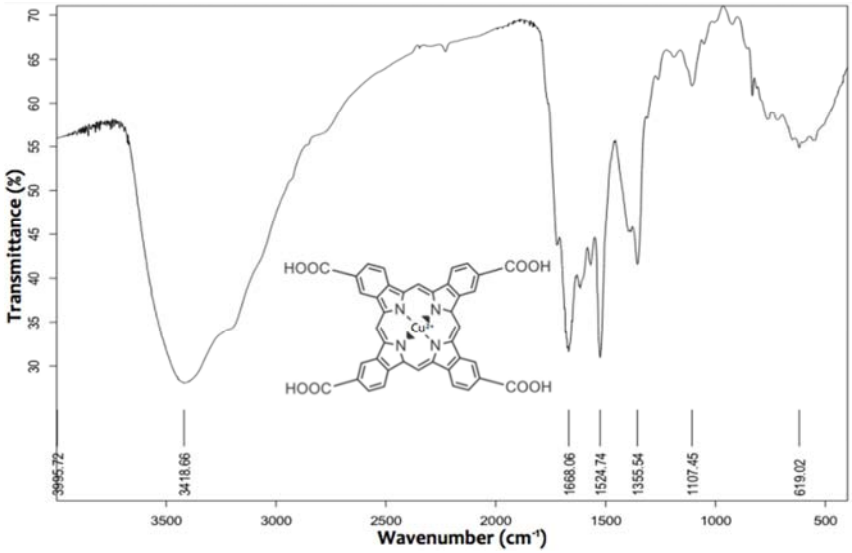

Fig. 3. *FTIR spectrum to PcTcCu synthesized in this work, PcTcCu chemical structure is given as inset image.*

3.3. UV–Vis Phthalocyanine Characterizations

Fig. 4 shows UV–Vis spectrum to T_cP_cCu dissolved in H_2SO_4 (c), spectrum shows typical Soret band around 320 nm, it corresponds to $\pi \rightarrow \pi^*$ transition; furthermore, broad bands located at 650 nm and 695 nm correspond to Q bands, these signals can be assigned to dimmer of phthalocyanines; P_cT_cMetal molecules can interact with each other through delocalized π electrons and hydrogen bonds [33]. The pH, concentration, temperature, solution polarity are most

important factors affecting aggregation [34], furthermore, phthalocyanines derivatives easily form dimmers even in dilute solutions [35].

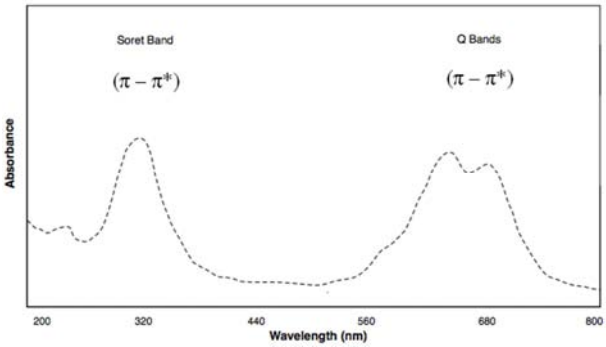

Fig. 4. *UV-Vis spectrum to PcTcCu synthesized in this work.*

3.4. Raman Sensitized Thin Films Characterization

Fig. 5 shows Raman spectrum to TiO_2, P_cT_cCu and TiO_2/P_cT_cCu. Results shows TiO_2 thin films shows typical Raman signals to anatase phase; symmetry modes corresponds to E_{1g} located at 144 cm^{-1}, 398 cm^{-1} and 520 cm^{-1}; E_{3g} to signal located at 639 cm^{-1}; these results corresponds to others reports [36]. Fig.4 shows typical signals of phthalocyanines after irradiation for using Laser of 780 nm under P_cT_cCu Powder, signal located at 1532 cm^{-1} can be assigned to bonding C_β –C_β vibration of pyrrole chemical group, signal located at 1330 cm^{-1} can be assigned to isoindole chemical group and signals located at 683 cm^{-1} and 746 cm^{-1} can be associated to symmetric and asymmetric distortions of macrocycle [37, 38]. Fig. 5 also shows Raman spectrum to TiO_2/P_cT_cCu. The main signal corresponded to the anatase phase. The final product TiO_2 PhthCu Raman spectrum indicates that no significant changes in the vibrational profile of the TiO_2 and PhthCu were occurred keeping their crystalline forms and characteristic symmetrical vibrational modes. Finally, Fig. 5 also shows Raman spectrum of TiO_2/P_cT_cCu, this spectrum shows an increase in the Raman intensity signals, this result can be assigned to SERS enhancements [39]. Results indicate that P_cTcCu is adsorbed on TiO_2 surface.

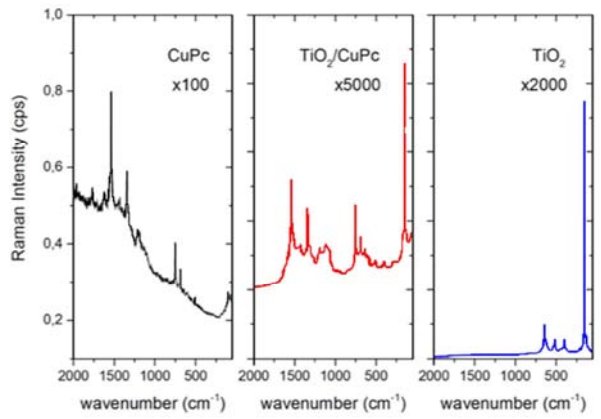

Fig. 5. *RAMAN spectra to TiO_2 and TiO_2/P_cT_cCu thin films and P_cT_cCu powder.*

3.5. Optical Sensitized Thin Films Characterization

Fig.6 shows reflectance diffuse spectrum to TiO_2 and TiO_2/P_cT_cCu thin films. TiO_2 spectrum does not show absorption at the visible range of electromagnetic spectrum (after 400 nm), due to the higher band gap of TiO_2 [40]. TiO_2/P_cT_cCu spectrum shows two bands located at 640 nm and 696 nm, however in this case the bands are not fully resolved; these two signals may be associated to transitions (n→π*), signals which are typical of phthalocyanines metal complexes [41].

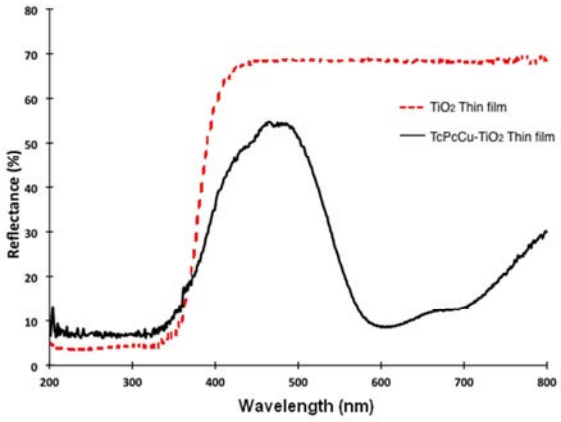

Fig. 6. *Reflectance diffuse spectrum to TiO_2 films and TiO_2/P_cT_cCu thin films.*

The diffuse reflectance spectra were analyzed through Kubelka Munk remission function through follow equation [42]:

$$F(R\alpha) = (1 - R\alpha)^2 / 2R\alpha \quad (1)$$

Where R_α is the reflectance; F (R_α) is an indicative of the absorbance of the sample at particular wavelength value and, it is proportional to the absorption constant of the material. We calculated the optical band gap by extrapolating the linear portion of the (F (R_α) $h\nu$)^2 vs. $h\nu$ plot on the x axis according to:

$$(F(R\alpha)\, h\nu)^2 = A(h\nu - Eg) \quad (2)$$

Where E_g is the band gap and A is a constant depending on the transition probability.

Fig. 7 shows that band gap of TiO_2 thin film was 3.28 eV, this corresponds to typical value of band gap energy of TiO_2 [43]; this result is according to Raman measurements presented before. Furthermore, results also show a redshift of absorption band for TiO_2/P_cT_cCu thin films, these films present a band gap energy of 1,58 eV, the broad absorption band at the visible region is attributed to P_cT_cCu molecules absorbed on TiO_2 surface. This represents a reduction of 51% in the band gap value, this result suggests, sensitization enhancement process TiO_2 photoresponse in visible range of electromagnetic spectrum [44]. Sensitization of TiO_2 thin films can permit to use visible region of electromagnetic spectrum to generate ROS.

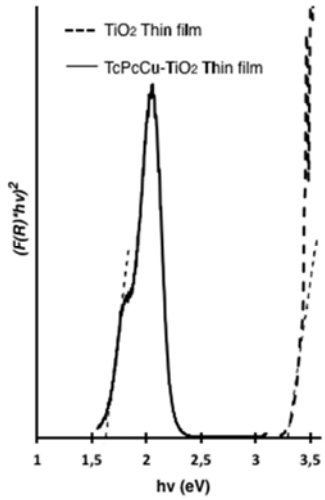

Fig. 7. *Plot of (F (R)hv)^2 vs. hv to both TiO_2 and TiO_2/P_cT_cCu thin films, band gapenergy value is indicated into x axis.*

3.6. SEM Analysis

Thin films morphology was studied through SEM analysis. In Figure 8a it can be seen a nanoporous structure. The nanostructure size is approximately 60 nm in all cases.

After sensitization process of aggregates on TiO_2 surface increase their size in around 100 nm (Fig. 8b), it is possible after adsorption process, P_cT_cCu support agglomeration process on TiO_2 surface, aggregation of phthalocyanines on TiO_2 thin films has been reported before [45].

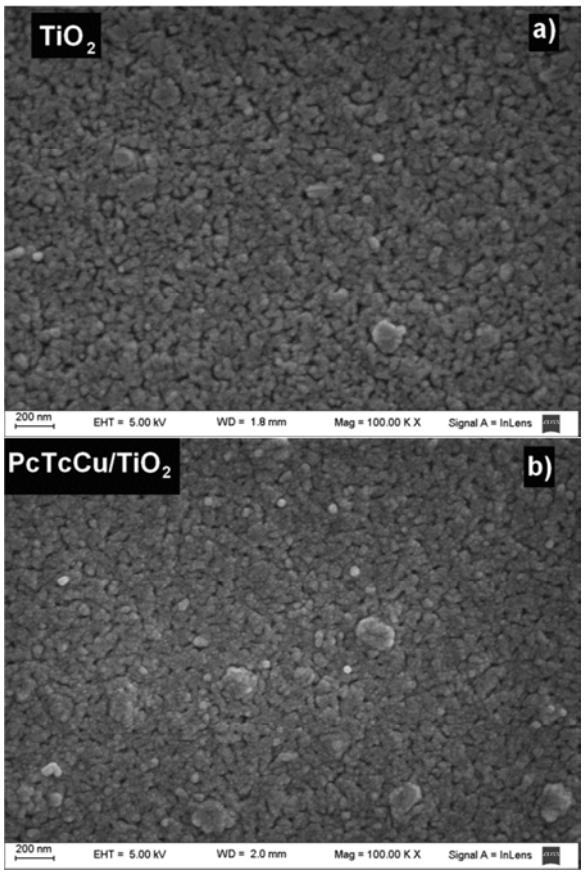

Fig. 8. *SEM images of a) TiO_2 and b) TiO_2/P_cT_cCu thin films.*

3.7. Antimicrobial Assay

Fig. 9 shows antimicrobial activity yield to TiO_2 and TiO_2/P_cT_cCu thin films. Under visible irradiation TiO_2 thin films did not show antibacterial activity after culture procedure; however, P_cT_cCu/TiO_2 had 81.5 % antimicrobial activity against to MRSA. After visible irradiation P_cT_cCu in basal state can be promoted to the first excited singlet state ($^1CuP_cT_c$*) three different events can occur: (1) electronic injection from LUMO $^1CuP_cT_c$* to conduction band of TiO_2 and subsequent generation of $O_{2\ (ad)}^{\bullet -}$ on TiO_2 surface; (2) generation $^1O_2$, through type reaction II [46]; (3) $O_{2\ (ad)}^{\bullet -}$ by photon induced electron transfer through mechanism named type I reaction [47]. Fig. 1 shows general scheme of this possible reactions. After irradiation ROS attack cell covering and they react to protein, lipids and nuclide acids; damages undergo by microorganism are irreversible [48].

Different reports have corroborated sensitizer must not be connected nor spread across into cell covering to destroy bacteria [49]. Results demonstrated high potential of Cu tetracarboxy–phenyl–phthalocyanine in development of antimicrobial surfaces.

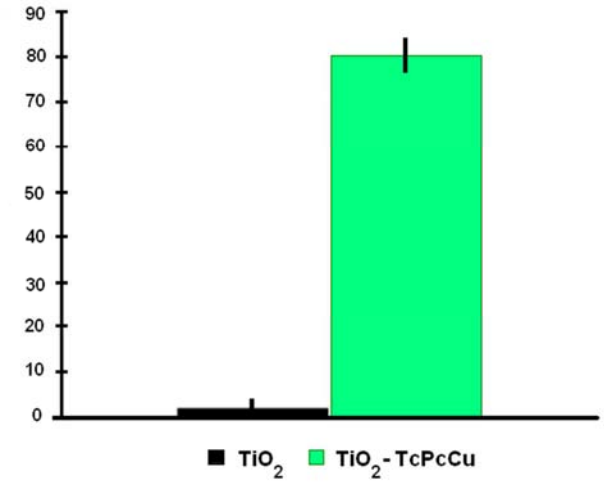

Fig. 9. *Antimicrobial activity to TiO_2 and TiO_2/P_cT_cCu thin films against to MRSA.*

4. Conclusions

In this work we deposited TiO_2 and TiO_2/P_cT_cCu thin films, P_cT_cCu was synthesized for using Achar method and besides, it was characterized by FTIR, UV–Vis and Raman spectroscopy. UV–Vis, Raman spectroscopy indicated SERS enhancements was presented after adsorption process of P_cT_cCu on TiO_2 thin films, furthermore optical results corroborated sensitization process improved photoactivity of TiO_2 thin films in visible range of electromagnetic spectrum. Antimicrobial effect under visible irradiation against MRSA showed T_cP_cCu/TiO_2 thin films reach 80.4% (+/3.4) of inhibition of MRSA growth after visible irradiation. Finally, our results indicated system TiO_2/T_cPcCu exhibited adequate germicidal properties against to MRSA bacteria.

References

[1] S. R. Harris et al., Evolution of MRSA during hospital transmission and intercontinental Spread, Science 327 (5964) (2010), 469–474. doi: 10.1101/gr.147710.112

[2] K. C. Ho, P. J. Tsai, Y. S. Lin, Y. C. Chen, Using biofunctionalized nanoparticles to probe pathogenic bacteria, Anal. Chem., 76 (24) (2004), 7162–7168. DOI: 10.1021/ac048688b

[3] K. Nawattanapaiboon et al., SPR-DNA array for detection of methicillin-resistant Staphylococcus aureus (MRSA) in combination with loop-mediated isothermal amplification, Biosens. Bioelectron. 74 (2015), 335–340. DOI: 10.1016/j. bios.2015.06.038

[4] C. Y. Wen, J. Hu, Z. L. Zhang, Z. Q. Tian, G. P. Ou, Y. L. Liao, Y. Li, M. Xie, Z. Y. Sun, D. W. Pang, One-step sensitive detection of Salmonella typhimurium by coupling magnetic capture and fluorescence identification with functional nanospheres, Anal. Chem., 85 (2) (2013), 1223–1230. DOI: 10.1021/ac303204q

[5] J. Paulsen, A. Mehl, A. Askim, E. Solligard, B. O. Asvold, J. K. Damas. Epidemiology and outcome of Staphylococcus aureus bloodstream infection and sepsis in a Norwegian county 1996–2011: an observational study, BMC Infect. Dis. 15 (2015), 116–126. DOI: 10.1186/s12879-016-1553-8.

[6] D. M. Underhill, Phagosome maturation: steady as she goes. Immunity 23 (2005) 343–346. iSSN 1074-7613.

[7] S. Rebiahi, D. Abdelouahid, M. Rahmoun, S. Abdelali, H. Azzaoui, Emergence of vancomycin-resistant Staphylococcus aureus identified in the Tlemcen university hospital (North-West Algeria). Médecine et maladies infectieuses. 41 (12) (2011) 646–651. doi:10.1016/j.medmal.2011.09.010

[8] M. Neginskaya, E. Berezhnaya, M. Rudkovskii, S. Demyanenko, A. Uzdensky. Photodynamic effect of Radachlorin on nerve and glial cells, Photodiagn. Photodyn. Ther. 11 (3) (2014) 357–364. doi:10.1117/12.2229929.

[9] G. Orellana, L. Villén, M. Jiménez-Hernández. Desinfección mediante fotosensibilizadores: Principios básicos. Solar Safe Water: Tecnologías solares para la desinfección y descontaminación del agua, ed J Blanco and MA Blesa, UNSAM, San Martín, Argentina. (2005) 237–251.

[10] X. H. Tao, Y. Guan, D. Shao, W. Xue, F. S. Ye, M. Wang, M. H. He. Efficacy and safety of photodynamic therapy for cervical intraepithelial neoplasia: A systemic review. Photodiagn. Photodyn. Ther. 11 (2) (2014) 104–112. doi: 10.1016/j. pdpdt.

[11] Y. Cheng, C. Burda. 2.01 - Nanoparticles for photodynamic therapy. Comprehensive Nanosc. Technol. (2011) 1-28. doi:10.1016/B978-0-12-374396-1.00071-4.

[12] T. Öztürk, H. Oner, A. O. Saatci, S. Kaynak. Low fluence photodynamic therapy combinations in the treatment of exudative agerelated macular degeneration. Intern. J. Ophthalmol. 5 (3) (2012) 377. doi:10.3980/j.issn.2222-3959.

[13] S. Banfi, E. Caruso, L. Buccafurni, R. Ravizza, M. Gariboldi, E. Monti, Zinc phthalocyanines-mediated photodynamic therapy induces cell death in adenocarcinoma cells, J. Organometal. Chem. 692 (6) (2007) 1269–1276. doi:10.1016/j.jorganchem.2006.11.028

[14] A. H. A. Machado, C. P. Soares, N. S. Da Silva, K. C. M. Moraes, Cellular and molecular studies of the initial process of photodynamic therapy in Hep2 cells using LED light source and two different photosensitizers, Cell Biology Intern. 33 (7) (2009) 785–795. DOI: 10.1016/j. cellbi.2009.04.011.

[15] J. P. Celli, B. Q. Spring, I. Rizvi, C. L. Evans, K. S. Samkoe, S. Verma, B. W. Pogue, T. Hasan, Imaging and photodynamic therapy: mechanisms, monitoring and optimization, Chemical Reviews 110 (5) (2010) 2795–2838. DOI: 10.1021/cr900300p.

[16] J. Paczkowskit, D. C. Neckers. Photochemical properties of rose bengal. 11. Fundamental Studies in Heterogeneous Energy Transfer. Macromolecules. 18 (12) (1985) 2412–2418. DOI: 10.1021/ma00154a013.

[17] M. Ochsner. Photophysical and photobiological processes in the photodynamic therapy of tumours. Journal of Photochemistry and Photobiology B: Biology 39 (1) (1997) 118.

[18] T. López, E. Ortiz, M. Álvarez, J. Navarrete, J. A. Odriozola, F. Martínez Ortega, E. A. Páez Mozo, Study of the stabilization of zinc phthalocyanine in sol gel TiO_2 for photodynamic therapy applications. Nanomedicine: Nanotechnology, Biology, and Medicine 6 (6) (2010) 777–785. doi: 10.1016/j. nano.

[19] A. Markowska-Szczupak, K. Ulfig, A. Morawski. The application of titanium dioxide for deactivation of bioparticulates: an overview. Catal. Today 169 (1) (2011) 249–257. doi:10.1016/j.cattod.2010.11.055.

[20] T. Fotiou, T. Triantis, T. Kaloudis, A. Hiskia, Evaluation of the photocatalytic activity of TiO_2 based catalysts for the degradation and mineralization of cyanobacterial toxins and water off-odor compounds under UV-A, solar and visible light. Chem. Eng. J. 261 (2015) 17–26. DOI: 10.1021/ie400382r.

[21] O. Modesto, P. Hammer, R. F. P. Nogueira, Gas phase photocatalytic bacteria inactivation using metal modified TiO_2 catalysts. J. Photochem. Photobiol A 253 (2013) 38–44. doi:10.1016/j.jphotochem.2012.12.016.

[22] A. Manassero, M. L. Satuf, O. M. Alfano. Evaluation of UV and visible light activity of TiO_2 catalysts for water remediation. Chem. Eng. J. 225 (2013) 378–386. DOI: 10.1016/j.cej.2013.03.097.

[23] L. Giribabu, K. Sudhakar, V. Velkannan. Phthalocyanines: potential alternative sensitizers to Ru (II) polypyridyl complexes for dye sensitized solar cells. Current Science 102 (7) (2012) 991–1000.

[24] Z. Chen, S. Zhou, J. Chen, L. Li, P. Hu, S. Chen, M. Huang. An effective zinc phthalocyanine derivative for photodynamic antimicrobial chemotherapy. J. of Luminescence 152 (2014) 103–107. doi:10.1016/j.jlumin.2013.10.067.

[25] P. Mikula, L. Kalhotka, D. Jancula, S. Zezulka, R. Korinkova, J. Cerny, et al. Evaluation of antibacterial properties of novel phthalocyanines against Escherichia coli–Comparison of analytical methods. Journal of Photochemistry and Photobiology B: Biology 138 (2014) 230–239. doi:10.1016/j.jphotobiol.2014.04.014.

[26] B. Achar, G. F., A. Parker, J. Keshavaya, Preparation and structural investigations of Cu (II),Co (II), Ni (II) and Zn (II) derivatives of 2,9,16,23 phthalocyanine tetracarboxylic acids. Indian J. Chem. 27 (1986) 411.

[27] B. N Achar. G. M. Fohlen, J. A. Parker, J. Keshavayya, Synthesis and structural studies of metal (II) 4,9,16,23-phthalocyanine tetraamines, Polyhedron 6 (6) (1987), 1463-1467. doi:10.1016/S0277-5387 (00)80910-9.

[28] P. M. Perillo, D. F. Rodríguez, Formation of TiO_2 Nanopores by Anodization of Ti-Films, Open Access Library Journal, 2014, 1, 1–9. http://dx.doi.org/10.4236/oalib1100630.

[29] A. Camacho, M. Giles, A. Ortegón, M. Palao, B. Serrano, O. Velázquez, Técnicas para el análisis microbiológico de alimentos. 2da Edición Facultad de Química, UNAM, (2009) 9 pages.

[30] S. Shrivastava, T. Bera, A. Roy, G. Singh, P. Ramachandrarao, D. Dash. Characterization of enhanced antibacterial effects of novel silver nanoparticles. Nanotechnol. 18 (22) (2007) 225103. doi:10.1088/0957-4484/18/22/225103.

[31] P. Zhao, Y. Song, S. Dong, L. Niua, F. Zhang. Synthesis, photophysical and photochemical properties of amphiphilic carboxyl phthalocyanine oligomers. Dalton Transactions, 32 (2009) 6327–6334. DOI: 10.1039/B904569D.

[32] Y. Gok, H. Z. Gok. Synthesis, characterization and spectral properties of novel zinc phthalocyanines derived from C2 symmetric diol. J. Molecular Structure 1067 (2014) 169–176. doi:10.1016/j.molstruc.2014.03.037.

[33] N. Touka, H. Benelmadjat, B. Boudine, O. Halimi, M. Sebais, Copper phthalocyanine nanocrystals embedded into polymer host: Preparation and structural characterization. J. Association of Arab Universities for Basic and Appl. Sci. 13 (1) (2013) 52–56. doi:10.1016/j.jaubas.2012.03.002.

[34] J. Nackiewicz, A. Suchan, M. Kliber. Octacarboxy phthalocyanines–compounds of interesting spectral, photochemical and catalytic properties. Chemik 68 (4) (2014) 369–376.

[35] B. Broz´ek–Płuska, I. Szymczyk, H. Abramczyk, Raman spectroscopy of phthalocyanines and their sulfonated derivatives, J. Mol. Struc. 744 (2005) 481–485. doi:10.1016/j.molstruc.2004.12.056.

[36] M. Vishwas, K. Narasimha Rao, R. Chakradhar, Influence of annealing temperature on Raman and photoluminescence spectra of electron beam evaporated TiO_2 thin films. Spectrochim. Acta Part A 99 (2012) 33–36.

[37] C. Jennings, R. Aroca, Ah–Mee Hor, R. O. Loutfy, Raman Spectra of Solid Films Mg, Cu and Zn Phthalocyanine Complexes. J. Raman Spectrosc. 15 (1) (1984) 34–37. DOI: 10.1002/jrs.1250150108.

[38] P. C. Lee and D. Meisel, Adsorption and Surface Enhanced Raman of Dyes on Silver and Gold Sols. J. Phys. Chem. 86 (17) (1982) 3391–3395. DOI: 10.1021/j100214a025.

[39] L. Yang, M. Gong, X. Jiang, D. Yin, X. Qin, B. Zhao W. Ruan. Investigation on SERS of different phase structure TiO_2 nanoparticles, J. Raman Spectrosc. 46 (3) (2015) 287–292. DOI: 10.1002/jrs.4645.

[40] U. Diebold. The surface science of titanium dioxide. Surf. Sci. Rep. 48 (5) (2003) 53–229. 10.1016/S0167-5729 (02)00100-0.

[41] K. Bayo, J. C. Mossoyan, G. V. Ouedraogo. Preparation and analysis by UV– Vis of zinc phthalocyanine complexes. Spectrochim. Acta Part A 60 (2004) 653–657. PMID: 14747091.

[42] A. B. Murphy, Bandgap determination from diffuse reflectance measurements of semiconductor films, and application to photoelectrochemical water splitting. Sol. Energy Mater. Sol. Cells 91 (2007) 1326–1337. doi:10.1016/j.solmat.2007.05.005.

[43] K. Gupta, R. P. Singh, A. Pandey. Photocatalytic antibacterial performance of TiO_2 and Ag doped TiO_2 against S. aureus. P. aeruginosa and E. Coli. Beilstein J. Nanotechnol. 4 (2013) 345–351. doi: 10.3762/bjnano.4.40.

[44] P. S. Batista, D. R.de Souza, R. V. Maximiano, N. M.Barbosa Neto, A. E. H. Machado. Quantum efficiency of hydroxyl radical formation in a composite containing nanocrystalline TiO_2 and zinc phthalocyanine, and the nature of the incident radiation. J. Mat. Sci. Res. 2 (3) (2013) 82–95. DOI: http://dx.doi.org/10.5539/jmsr.v2n3p82.

[45] R. Ashokkumar, A. Kathiravan, P. Ramamurthy. Zn phthalocyanine functionalized Nanometal and nanometal–TiO_2 hybrids: aggregation behavior and excited state dynamics. Phys. Chem. Chem. Phys. 16 (2014) 14139–14149. DOI: 10.1039/C4CP00695J.

[46] G. Schneider, D. Wohrle, W. Spiller, J. Stark, G. Schulz Ekloff, Photooxidation of 2-mercaptoethanol by various water-soluble phthlalocyanines in aqueous alkaline solution under irradiation with visible light, Photochem. Photobiol. 60 (1994) 333–342. DOI: 10.1111/j.1751-1097.1994.tb05112.

[47] V. Iliev, A. Mihaylova, L. Bilyarska. Photooxidation of phenols in aqueous solution, catalyzed by mononuclear and polynuclear metal phthalocyanine complexes. J. Mol. Cat. A: Chem. 184 (2002) 121–130. doi:10.1016/S1381-1169 (01) 00520-9.

[48] A. Hegueta, M. E. Jimenez, F. Montero, E. Oliveros, G. Orellana, Singlet oxygen mediated DNA photocleavage with Ru (II) polypyridyl complexes, J. Phys. Chem. B 106 (2002) 4010–4017. DOI: 10.1021/jp013542r.

[49] S. A. Bezman, P. A. Burtis, T. P. J. Izod, M. A. Thayer, Photodynamic inactivation of *E. coli* by rose Bengal immobilized on polystyrene beads, J. Photochem. Photobiol. 28 (1978) 325–329. DOI: 10.1111/j.1751-1097.1978.tb07714.x.